Coherent Pulse Propagation and the Dynamics of Rydberg Wave Packets

J. Arlt, C. Weiss, G. Torosyan, and R. Beigang
University of Kaiserslautern, 67663 Kaiserslautern, Germany
(Received 2 July 1997)

The pulse reshaping of femtosecond laser pulses tuned to Rydberg transitions of strontium vapor is observed experimentally. We show theoretically that their shape closely reflects the dynamics of Rydberg wave packets induced by the pulses. The decay and compression of Rydberg wave packets excited by both Fourier limited and chirped fs pulses is presented. [S0031-9007(97)04796-0]

PACS numbers: 32.80.Qk, 32.80.Rm, 42.25.Bs

Laser pulses with a duration shorter than the transverse relaxation time of a dispersive medium propagate in a coherent fashion. If the pulses are weak, their coherent propagation can simply be described by means of linear dispersion theory [1]. The reshaping of such small-area pulses during propagation has been observed in many different systems in the visible, infrared, and terahertz region of the electromagnetic spectrum [2–4]. The pulse shape for pulses of ultraviolet light has also been predicted [5] recently.

The short duration of femtosecond laser pulses corresponds to a large spectral width. When such a pulse is tuned to Rydberg transitions of an atom or molecule, it can excite more than one level simultaneously. This leads to a coherent superposition of Rydberg states and, thus, to the formation of Rydberg wave packets [6,7]. The formation and dynamics of these wave packets has been investigated by means of various experimental techniques such as the pump-probe method used by Yeazell *et al.* [8]. In this paper, we show theoretically that the dynamics of the Rydberg wave packet is reflected in the shape of the propagating pulse. This enables us, in particular, to interpret the experimentally observed reshaping of chirped and unchirped femtosecond pulses in terms of a contracting and decaying wave packet.

In the following, we consider only pulses which are so weak that they do not deplete the atomic ground state significantly and, therefore, linear dispersion theory can be used to describe the propagating pulse. As Crisp [1] has shown, the pulse shape can then be calculated explicitly. If the initial pulse is written as a slow-varying complex valued envelope $\mathcal{E}(t,z)$ modulating a sinusoidal carrier

$$E(t,0) = \mathcal{E}(t,0)e^{-i\omega t}, \tag{1}$$

the pulse envelope after propagating a distance z through a dispersive medium is given by [1]

$$\mathcal{E}(t,z) = \frac{1}{2\pi}\int_{-\infty}^{\infty}\hat{\mathcal{E}}(\nu,0) \times \exp\left[-i\nu\left(t - \frac{\eta}{c}z\right) - A(\nu)z\right]d\nu\,. \tag{2}$$

Here, $\hat{\mathcal{E}}(\nu,0)$ and η denote the Fourier transform of the pulse envelope which corresponds to the spectrum of the initial pulse and the frequency independent refractive index, respectively. The interaction between light and atoms is expressed in the function $A(\nu)$, which is essentially the complex refractive index $\tilde{n}(\omega')$ of a single resonance convoluted with the inhomogeneous line shape $g(\nu)$:

$$A(\nu) = -i\frac{\nu}{\eta c}\int_{-\infty}^{\infty} g(\Delta)[\tilde{n}(\nu - \Delta) - 1]\,d\Delta\,. \tag{3}$$

Although Eq. (2) was initially derived on the basis of the model of a two-level atom, it can be easily generalized to multilevel atoms. The equations remain unchanged and the only difference is that now the plasma dispersion function is used to calculate the complex refractive index:

$$\tilde{n}(\omega') - \eta = \frac{\omega_p^2}{4\eta\omega'}\sum_n \frac{f_n}{\omega_n - \omega' - i\gamma_n/2}\,, \tag{4}$$

where ω_n, γ_n, and f_n are the excitation frequencies to Rydberg states with principle quantum number n, the damping constant, and the oscillator strength, respectively.

Figure 1 shows the result of a numerical calculation based on Eqs. (2) and (4) for a pulse which is in resonance with several Rydberg transitions. The most characteristic feature is the sequence of equidistant peaks. This can be easily associated with the dynamics of a radial Rydberg wave packet induced by the propagating pulse [7]. The

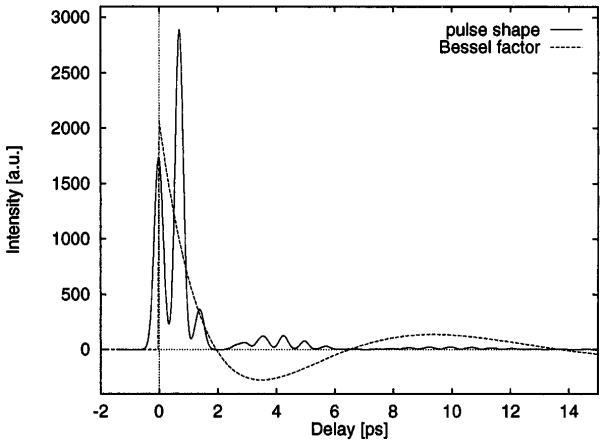

FIG. 1. Pulse reshaping by resonant Rydberg transitions.

 0031-9007/97/79(24)/4774(4)$10.00

fact that Rydberg levels are not equally spaced leads to the broadening and eventual decay of the wave packet.

Although the connection to the dynamics of the wave packet is apparent in the actual pulse shape, this is not obvious from Eq. (2). In the following, we establish this connection more explicitly. The wave packet dynamics follows the expectation value of the induced electric dipole moment between the ground and the excited Rydberg states. The electric dipole element is given by

$$\mu(t) = \frac{i}{\hbar} \sum_n |\mu_n|^2 \int_0^\infty \mathcal{E}(t - t', z) \times \exp[-i(\omega_n - \omega)t'] \, dt' \exp(-i\omega t), \quad (5)$$

where $\mathcal{E}(t, z)$ is the envelope of the input pulse and μ_n and ω_n are the matrix element and frequency for the $\Delta l = 1$ transitions, respectively. The induced dipole moment is proportional to the radial expectation value of the wave packet.

Equation (5) has to be compared with the field envelope given by Eq. (2), which will be transformed until its relation to the expectation value of the induced dipole moment becomes apparent.

If one expands the factor $\exp[-A(\nu)z]$ as a power series and uses the convolution theorem, Eq. (2) can be written as

$$\mathcal{E}(t, z) = \sum_{m=0}^{\infty} \frac{(-z)^m}{m!} \times \int_{-\infty}^{\infty} \mathcal{E}\left(t' - \frac{\eta}{c} z, 0\right) \tilde{A}_m(t - t') \, dt', \quad (6)$$

where $\tilde{A}_m(t)$ is the Fourier transform of the mth power of $A(\nu)$:

$$\tilde{A}_m(t) = \int_{-\infty}^{\infty} [A(\nu)]^m e^{-i\nu t} \, d\nu . \quad (7)$$

If one neglects the inhomogeneous broadening and assumes that the spacing between the different resonances is large compared to their width, $\tilde{A}_m(t)$ can be calculated explicitly:

$$\tilde{A}_0(t) = \delta(t), \quad (8)$$

$$\tilde{A}_m(t) = \begin{cases} 0, & t \le 0, \\ \left(\frac{\omega_p^2}{4\eta c}\right)^m \sum_n f_n^m \frac{t^{m-1}}{\Gamma(m)} e^{-\gamma/2 t} e^{-i(\omega_n - \omega)t}, & t > 0. \end{cases} \quad (9)$$

In Eq. (9), it is also assumed that the damping constant γ is equal for all excited Rydberg states. If this expression is used in Eq. (6), one finds the first term ($m = 0$) reproduces the (time-shifted) input envelope. This is the only term present if the pulse propagates in nondispersive media. Only the higher contributions ($m > 0$) are due to the interaction between the pulse and the atoms. The expression for these higher contributions to the pulse envelope can be simplified by realizing that (see [9])

$$\sum_{m=1}^{\infty} (-\alpha_n z)^m \frac{\tau^{m-1}}{m!\,(m-1)!} = -\sqrt{\frac{\alpha_n z}{\tau}} J_1(2\sqrt{\alpha_n z \tau}), \quad \text{with } \alpha_n = \frac{f_n \omega_p^2}{4\eta c}, \quad (10)$$

where $J_1(x)$ is the first order Bessel function and α_j is the absorption length. The relevant part of the envelope can then be expressed as

$$\mathcal{E}_{\mathrm{WP}}(t, z) = \mathcal{E}(t, z) - \mathcal{E}\left(t - \frac{\eta}{c} z, 0\right) = -\sum_j \int_0^\infty \sqrt{\frac{\alpha_n z}{\tau}} J_1(2\sqrt{\alpha_n z \tau}) \times \mathcal{E}\left(t - \frac{\eta z}{c} - \tau, 0\right) e^{-[\gamma/2 + i(\omega_n - \omega)]\tau} \, d\tau . \quad (11)$$

Now the relation to the induced dipole moment [Eq. (5)] and, thus, the radial expectation value are clearly visible. Both expressions involve a sum of similar integrals but in Eq. (11) each term is modified by a different factor $\sqrt{\alpha_n z/\tau}\, J_1(2\sqrt{\alpha_n z \tau})$. These modifying factors are also included in Fig. 1.

The uv pulses used for the pulse propagation experiments in strontium were generated via frequency quadrupling of the radiation of a cw mode-locked Ti:sapphire laser. The uv pulses obtained with our experimental setup have typical durations between 200 and 400 fs and are still close to Fourier limited sech^2 pulses. The average power is less than 2 mW, which corresponds to a pulse energy of 24 pJ. For transitions to Rydberg states with $n \ge 8$, the pulse area is $\Theta \le 3.5 \times 10^{-3}$ so that we are well within the small-area limit. By tuning the Ti:sapphire laser, we covered the wavelength range between 210 and 250 nm.

With this tuning range, it is possible to excite strontium transitions Sr $5s^2\ {}^1\mathrm{S}_0$-$5snp\,{}^1P_1$ from $n = 8$ up to the ionization limit. The strontium vapor was produced in a stainless steel heat pipe oven which was operated at a temperature of 800 °C and a pressure of 2 mbar. The active length of the heat pipe was about 6 cm. After passage of the uv pulse through the Sr vapor, the modified pulse shape was determined via an optical cross correlation by difference frequency mixing of the uv pulse with the time delayed pulse at the fundamental frequency in a 100 μm thick beta barium borate crystal. The time resolution was determined by the pulse length of the fundamental pulse which was around 150 fs.

Figure 2 shows some of the measured pulse shapes for different wavelengths. The front-most graph shows the pulse shape when only two transitions are resonant ($n = 21$ and $n = 22$). For the following measurements, the central frequency of the pulse is slightly increased while the duration and the spectrum of the initial pulses stay

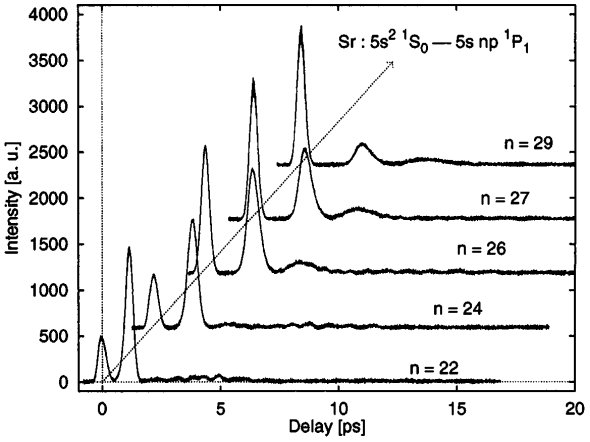

FIG. 2. Pulse reshaping by resonant Rydberg transitions for different wavelengths.

essentially the same. Since the spacing between Rydberg transitions decreases with higher frequencies ($\propto n^{-3}$), this implies that there are more levels resonant simultaneously for the higher frequencies.

The shown pulse shapes reflect several characteristics of the Rydberg wave packet induced by them. The first peak always represents the initial pulse which is weakened but not broadened. The following peak marks the time when the wave packet returns to the core. Obviously, this orbital period of the wave packet increases as one goes to higher transitions. The measured time separation between the two leading peaks is in good agreement with the classical orbital period

$$T_n = \frac{(n^*)^3}{2R_{\mathrm{Sr}}c}, \tag{12}$$

where n^* is the effective quantum number and R_{Sr} is the Rydberg constant for strontium.

The second feature of Rydberg wave packets noticeable in the pulse shape is their spreading. The decay of the wave packets is fairly rapid and becomes faster for higher transitions. The second peak is already broadened considerably compared to the initial pulse duration. The third peak after twice the orbital period is only distinct for higher transitions.

The decay of the wave packet can be influenced by the frequency characteristics of the exciting pulses [10,11]. Using uv pulses with a linear frequency chirp, the decay will be accelerated or slowed down depending on the sign of the chirp. With a linearly down-chirped excitation pulse, where the central frequency decreases with time according to

$$\omega(t) = \omega_0 - bt, \tag{13}$$

transitions with higher frequencies (i.e., higher n) will be excited before the transitions with lower frequencies. But the higher transitions have a longer orbital period [Eq. (12)]; they are "slower." After this initial period of contraction, the wave packet will obviously decay again.

If one uses an up-chirped pulse to excite a wave packet, the decay is accelerated and, typically, one does not even see the second peak but a fairly random looking pulse shape.

For the measurements shown in Fig. 3, a pulse of a Fourier limited duration of 300 fs is down-chirped using a combination of two LiF prisms with a spatial separation of 2.3 m. The pulse duration is increased to 650 fs. The

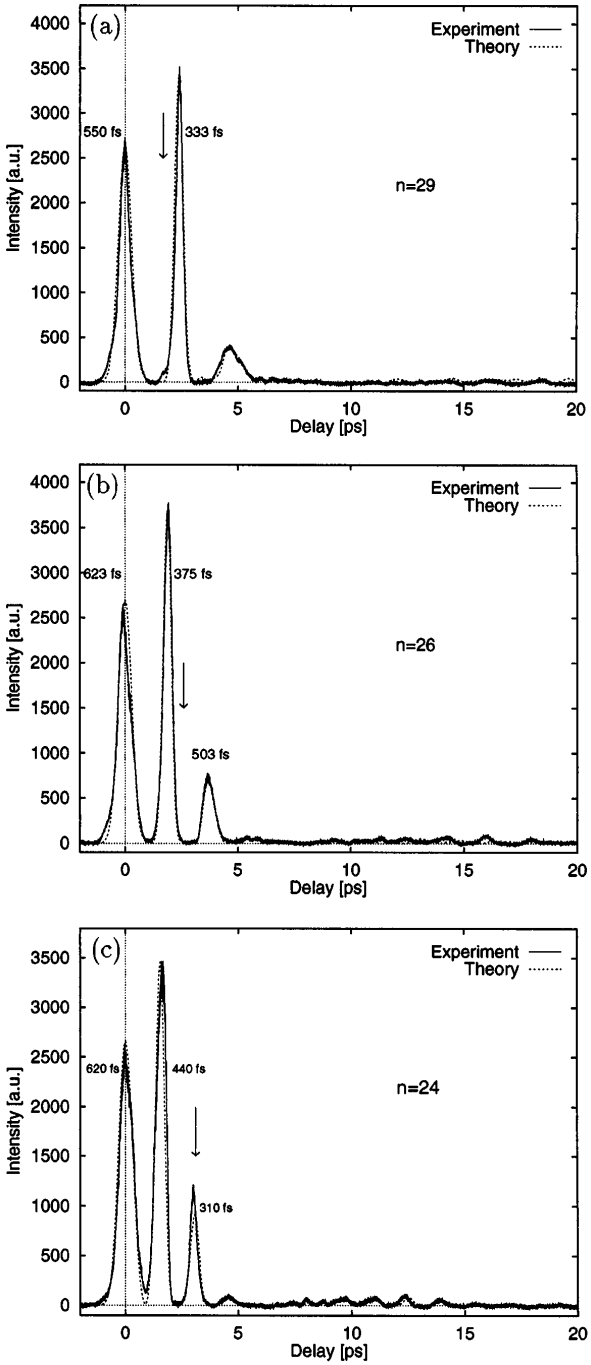

FIG. 3. Chirped Rydberg wave packets. The arrow indicates the temporal position of maximum compression of the wave packet.

figure shows the reshaped pulse for three different central frequencies corresponding to the transitions $n = 24$, 26, and 29. The pulse shape only gives us information about the wave packet when this is close to the core, i.e., only at multiples of the orbital period. To obtain optimum compression (i.e., the pulse duration is reduced to the Fourier limit of the exciting pulse), one can either adjust the chirp of the initial pulse for a given transition or keep the chirp fixed and look for the transition frequency which yields optimum compression. For experimental reasons, we kept the chirp of the uv pulses fixed.

In Fig. 3(a), the wave packet is centered around the transition $n = 29$. Here, the compression is very fast and after one orbital period the wave packet is already expanding again. Nevertheless, it is still considerably shorter than the excitation pulse and the third peak is clearly more distinct than in the unchirped case. In Fig. 3(b), the compression is slightly too slow to observe the optimum compression after one orbital period. Optimum compression is somewhere in between the second and third peaks. Finally, Fig. 3(c) shows optimum compression after the second orbital period. The third peak has a duration which corresponds to the Fourier limited excitation pulse ($\tau = 310$ fs) and even a fourth peak becomes visible.

The propagation and pulse reshaping of uv fs pulses in a multilevel atomic system is reported. The reshaped pulses reflect the dynamics of wave packets as was shown theoretically. Using Sr vapor and tuning the uv pulses to Rydberg state transitions, the wave packet dynamics was experimentally observed for the first time, to our knowledge, in the reshaped fs pulses. Excitation with linearly down-chirped pulses leads to a compression of the wave packets which was also observed experimentally. Using linear dispersion theory adopted for multilevel systems, good agreement between experiment and theory was obtained.

This work was supported by the Deutsche Forschungsgemeinschaft DFG.

[1] M. D. Crisp, Phys. Rev. A **1**, 1604 (1970).
[2] J. E. Rothenberg, D. Grischkowsky, and A. C. Balant, Phys. Rev. Lett. **53**, 552 (1984).
[3] H. J. Hartmann and A. Laubereau, Opt. Commun. **47**, 117 (1983).
[4] H. Harde and D. Grischkowsky, Inst. Phys. Conf. Ser. **126**, 217 (1992).
[5] I. P. Christov, Opt. Commun. **113**, 530 (1995).
[6] J. Parker and C. R. Stroud, Jr., Phys. Rev. Lett. **56**, 716 (1986).
[7] G. Alber, H. Ritsch, and P. Zoller, Phys. Rev. A **34**, 1058 (1986).
[8] J. A. Yeazell, M. Mallalieu, and C. R. Stroud, Jr., Phys. Rev. Lett. **64**, 2007 (1990).
[9] I. S. Gradshteyn, *Tables of Integrals, Series and Products* (Academic Press, New York, 1965).
[10] D. W. Schumacher, J. H. Hoogenraad, D. Pinkos, and P. H. Bucksbaum, Phys. Rev. A **52**, 4719 (1995).
[11] B. Kohler *et al.*, Phys. Rev. Lett. **74**, 3360 (1995).